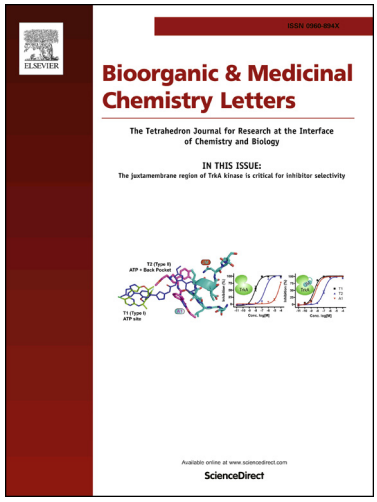

Discovery and structure-activity relationship studies of *N*-substituted indole derivatives as novel Mcl-1 inhibitors

Shenglin Luan, Qi Ge, Yedong Chen, Mingyang Dai, Jinyu Yang, Kun Li, Dan Liu, Linxiang Zhao

PII: S0960-894X(17)30263-9
DOI: http://dx.doi.org/10.1016/j.bmcl.2017.03.028
Reference: BMCL 24780

To appear in: *Bioorganic & Medicinal Chemistry Letters*

Received Date: 10 January 2017
Revised Date: 18 February 2017
Accepted Date: 14 March 2017

Please cite this article as: Luan, S., Ge, Q., Chen, Y., Dai, M., Yang, J., Li, K., Liu, D., Zhao, L., Discovery and structure-activity relationship studies of *N*-substituted indole derivatives as novel Mcl-1 inhibitors, *Bioorganic & Medicinal Chemistry Letters* (2017), doi: http://dx.doi.org/10.1016/j.bmcl.2017.03.028

Discovery and structure-activity relationship studies of *N*-substituted indole derivatives as novel Mcl-1 inhibitors

Shenglin Luan[a], Qi Ge[a], Yedong Chen[a], Mingyang Dai[a], Jinyu Yang[a], Kun Li[a], Dan Liu[a]*, Linxiang Zhao[a]*

[a] Key Laboratory of Structure-Based Drugs Design & Discovery of Ministry of Education, Shenyang Pharmaceutical University, Shenyang 110016, China

* Corresponding authors:

E-mail address: linxiang.zhao@vip.sina.com (Linxiang Zhao); sammyld@163.com (Dan Liu).

Tel.: +86 024 43520221;

Abstract

Myeloid cell leukemia-1 (Mcl-1) is an important antiapoptotic protein functioning through protein-protein interactions. We discovered **LSL-A6** (2-((2-carbamoyl-1-(3-(4-methoxyphenoxy)propyl)-1*H*-indol-6-yl)oxy)acetic acid) with a novel *N*-substituted indole scaffold to interfere Mcl-1 binding as a novel Mcl-1 inhibitor. Molecular modeling indicated that this compound binds with Mcl-1 by interaction with P2 and R263 hot-spots. Structure modification focused on several moieties including indole core, hydrophobic tail and acidic chain were conducted and structure-activity relationship was analyzed. The most potent compound **24d** which exhibited K_i value of 110 nM for interfering Mcl-1 binding was obtained after hit-to-lead modification.

Keywords: Apoptosis; Bcl-2; Mcl-1; Structure-based design

Evasion of apoptosis is a hallmark of cancer and a contributor of resistance to current chemotherapies. [1, 2] The B-cell lymphoma-2 (Bcl-2) family of proteins are the vital regulators of mitochondrial apoptosis pathway, [3, 4] which include three types of proteins: the antiapoptotic proteins (Bcl-2, Bcl-x_L, Bcl-w, Mcl-1 and Bfl-1/A1), the proapoptotic proteins (Bak, Bax and Bok)

and the BH3-only proteins (Bim, Puma, Noxa *etc.*). [5] Overexpression of antiapoptotic Bcl-2 proteins was disclosed in many cancers including leukemia, melanoma, lung, breast, prostate, pancreatic, ovarian and cervical cancers. [6, 7]

Interfering interactions of Bcl-2 antiapoptotic proteins and proapoptotic proteins to induce apoptosis becomes a promising anticancer strategy. Potent Bcl-2 and/or Bcl-x_L inhibitors have been developed in the last decades. Navitoclax (ABT-263), binding to Bcl-2, Bcl-x_L and Bcl-w, has provided promising results in clinical trials despite of the on-target side-effect thrombocytopenia (caused by inhibition of Bcl-x_L). [8, 9] More recently, the selective Bcl-2 inhibitor venetoclax (ABT-199) avoiding the side effect of Bcl-x_L inhibition of navitoclax has been approved by FDA for the treatment of chronic lymphocytic leukemia with 17p deletion and at least one prior therapy.[10, 11]

Neither venetoclax nor navitoclax has Mcl-1 inhibitory activity and the high Mcl-1 levels cause the loss of efficacy of both agents in several types of tumors. [12, 13] Moreover, several publications showed that Mcl-1 protein overexpression is a critical factor conferring resistance to navitoclax and other widely used anticancer agents. [12, 14-16] Decreased or silenced Mcl-1 expression has shown tumor growth inhibitory effects and/or enhanced chemo-sensitivity in cancer cells. [17] Indirect inhibition of Mcl-1 through Noxa upregulation could effectively induce apoptosis in acute myeloid leukemia. [18] Mcl-1 is being considered as an attractive anticancer target for developing therapeutics.

With significant effort has been devoted towards the development of Mcl-1 inhibitors, numbers of small molecules comprising diverse chemotypes have been reported and none of authentic Mcl-1 inhibitors enters the clinical trials. [19-32] Thus, development of novel Mcl-1 inhibitors still represents an unmet clinical need. Here we describe a hit-to-lead optimization and related SAR studies of Mcl-1 inhibitors based on a novel *N*-substituted indole scaffold.

(**Figure 1** should be listed here)

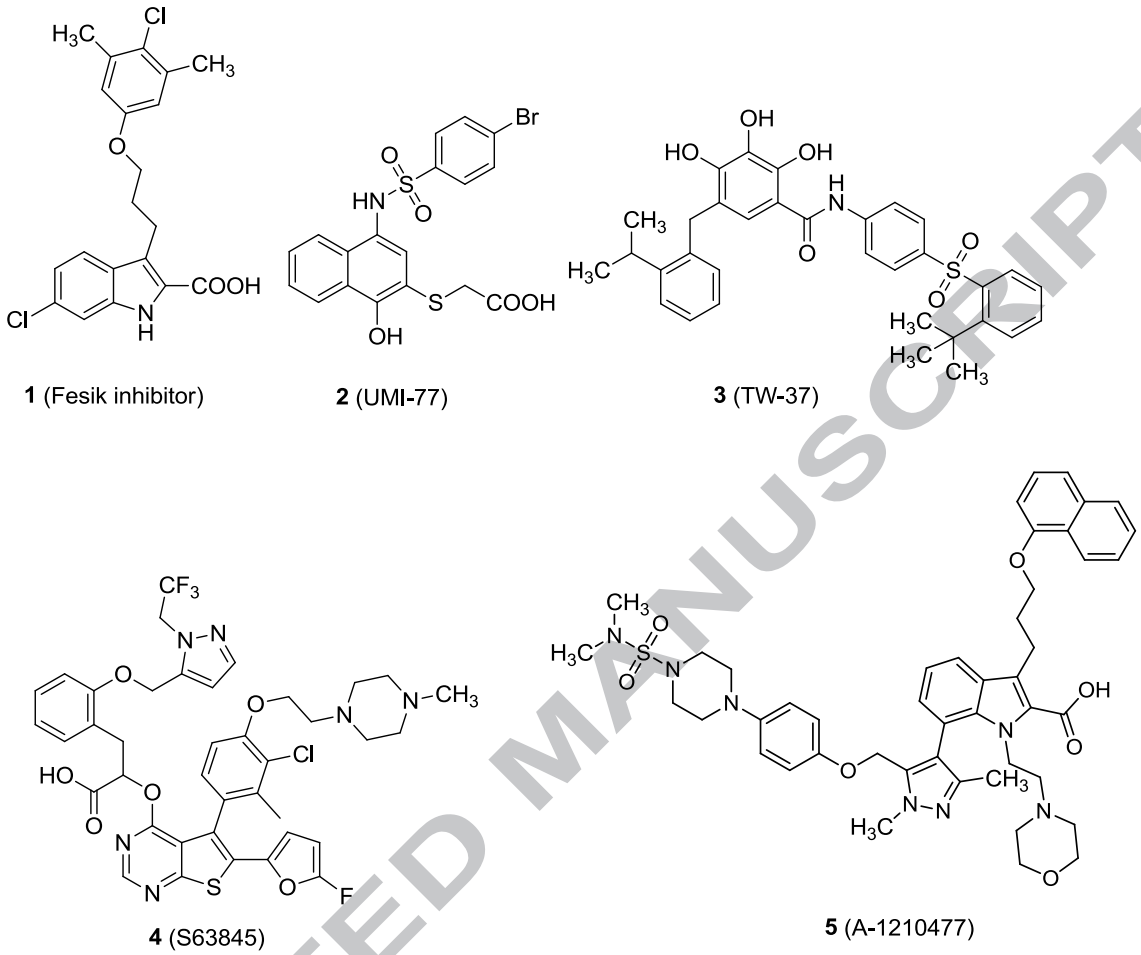

Figure 1. The recently reported Mcl-1 inhibitors.

A small in-house compound library comprising synthetic molecules and natural product derivatives were screened for inhibitory activity of Mcl-1 using fluorescence polarization binding assay (FP assay). Bid-BH3 peptide was labeled with fluorescein as the probe to monitor the competitive binding of these compounds to Mcl-1. The traditional Mcl-1 inhibitor (−)-gossypol was used as control. **LSL-A6** (**14a**) bearing *N*-substituted indole scaffold was one of validated hits with K_i value of 7.78 μM. To guide the further optimization of hit compound **14a**, molecular docking studies were performed using the crystal structure (PDB code: 4HW3) of Mcl-1 in complex with a reported inhibitor (**1, Figure 1**). [24] A low energy docking solution was depicted in **Figure 2**. The docking result reveals that compound **14a** binds with Mcl-1 protein by the occupation of P2 pocket and the formation of salt bridge with R263, the two most important hot-spots of Mcl-1 as reported. [24, 33] In order to facilitate description, compound **14a** was divided into

three moieties including indole core, hydrophobic tail and acidic chain (**Figure 2**). In detail, the hit compound **14a** interacts with R263 through a salt bridge mediated by carboxyl group and a hydrogen bond by oxygen atom on the acidic chain. The 1*H*-indole-2-carboxamide scaffold occupies the upper P2 pocket, while the 4-methoxyphenyl on hydrophobic tail inserts into the bottom of P2 pocket through a saturated carbon chain. Both of these two moieties could interact with P2 hydrophobic residues that include M250, V253 and F270. Based on the predicted binding mode, we made further optimization of hit compound **14a** to develop potent Mcl-1 inhibitors.

(**Figure 2** should be listed here)

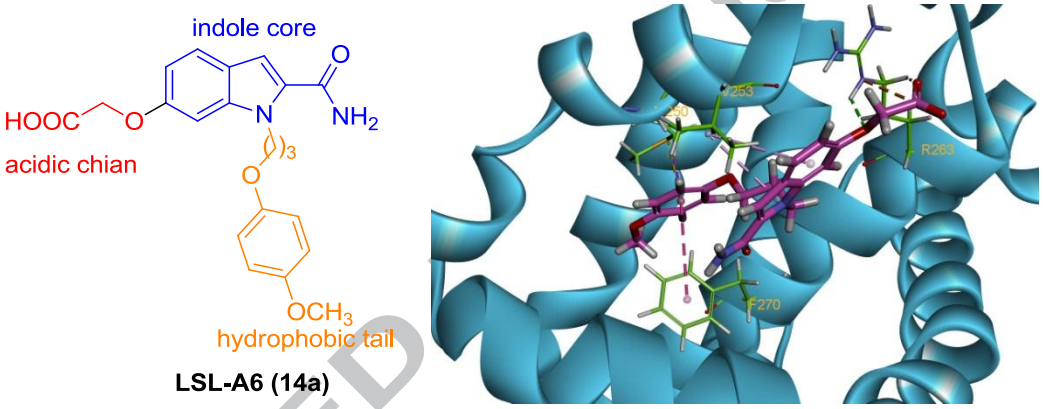

Figure 2. The structure and predicted binding mode of **LSL-A6** (**14a**) bound to Mcl-1 (PDB: 4HW3). Pink carbons; heteroatoms colored by atom type; the amino acid side chains interacting with ligand were colored as green. The pink dashed lines present hydrophobic interactions; the orange dashed lines present salt bridges; the green dashed lines present hydrogen bonds.

All the side chains and indole derivatives were prepared according to methods outlined in **Schemes 1–2**. Experimental details are described in the *Supplementary Information*. Side chains **7a-7m** were prepared by substitution reaction of dibromoethane or dibromopropane with commercial phenols or thiophenols. The synthetic route employed for preparation of the 6-hydroxy-1*H*-indole-2-carboxamide (**11a**) was reported previously and similar routes were used to prepare **11b-11d**. [34] By nucleophilic substitution reactions of **11a-11d** with ethyl bromoacetate or methyl *o*-(bromomethyl)benzoate, key intermediates **12a-12e** were synthesized. Intermediates **13a-13i** were obtained via another nucleophilic substitution of **12a-12e** with various side chains (**7a-7d** and **7j)** which then hydrolyzed under base condition to afford target compounds **14a-14i**.

Compounds **17a-17p**, **24a-24j** were obtained by a simplified route including just two easy substitution reactions and one hydrolysis reaction. Briefly, commercial hydroxyindoles successively reacted with ethyl bromoacetate (or ethyl 2-bromobutyrate and methyl bromomethylbenzoates) and side chains to afford ester analogues **16a-16p** (or **23a-23j**) which were then converted to target compounds by general hydrolyzed condition. Specially, the hydroxyl derivative **18** was achieved through a reduction of compound **16j** with lithium aluminum hydride. Compound **21** was synthesized through similar procedures with indole-6-carboxylic acid as starting material in three-step feasible reactions including esterification, nucleophilic substitution and hydrolysis. Compounds **20a-20c** were prepared through *N*-alkylation reactions with different indoles.

(**Scheme 1** should be listed here)

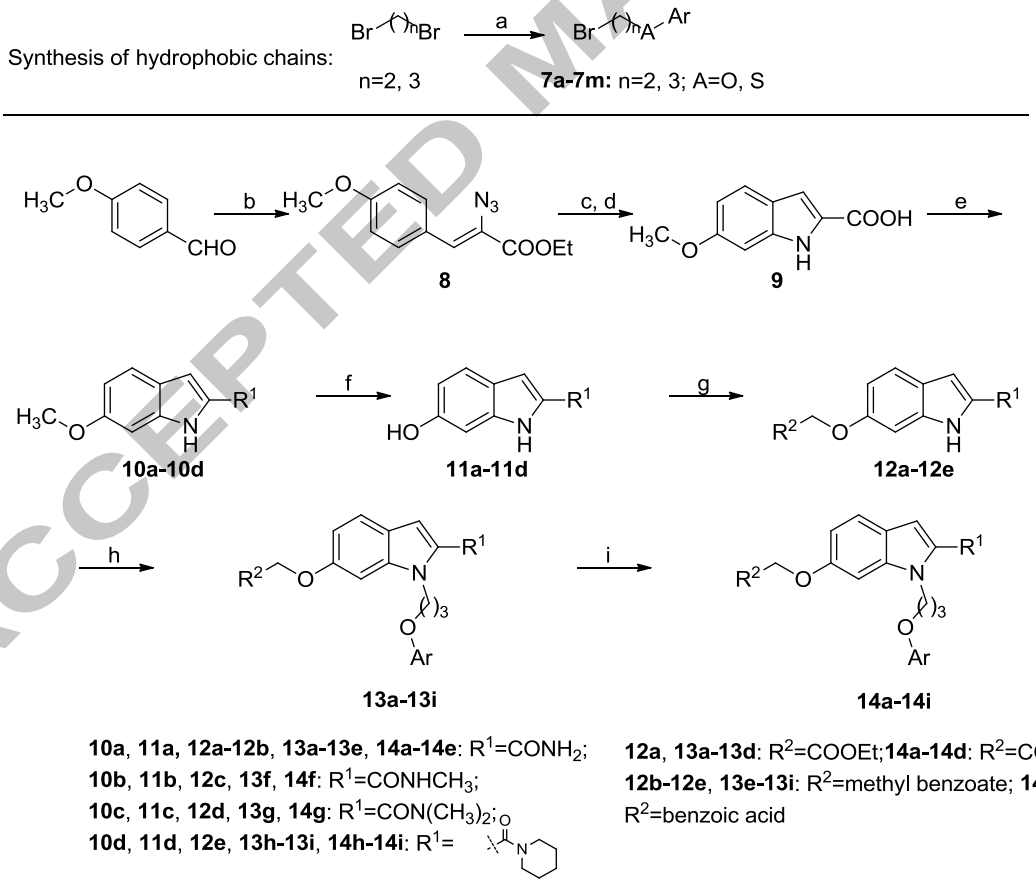

Scheme 1. Synthetic routes of side chains **7a-7m** and 2-substituted indole derivatives **14a-14i**
Reagents and conditions: a) substitued phenol or phenthiol, K_2CO_3, MeCN, reflux; (b) ethyl azidoacetate, C_2H_5ONa, C_2H_5OH, -5-0 ^oC; (c) xylene, 135 ^oC; (d) NaOH/H_2O, CH_3OH, reflux; (e) various amine, HOBt, EDCI, Et_3N, CH_2Cl_2, r.t.; (f) BBr_3, CH_2Cl_2, -30 ^oC; (g) $BrCH_2COOEt$ or methyl *o*-(bromomethyl)benzoate, Cs_2CO_3, MeCN, r.t.; (h) side chains, Cs_2CO_3, MeCN, reflux; (i) LiOH, THF/H_2O, r.t..

(**Scheme 2** should be listed here)

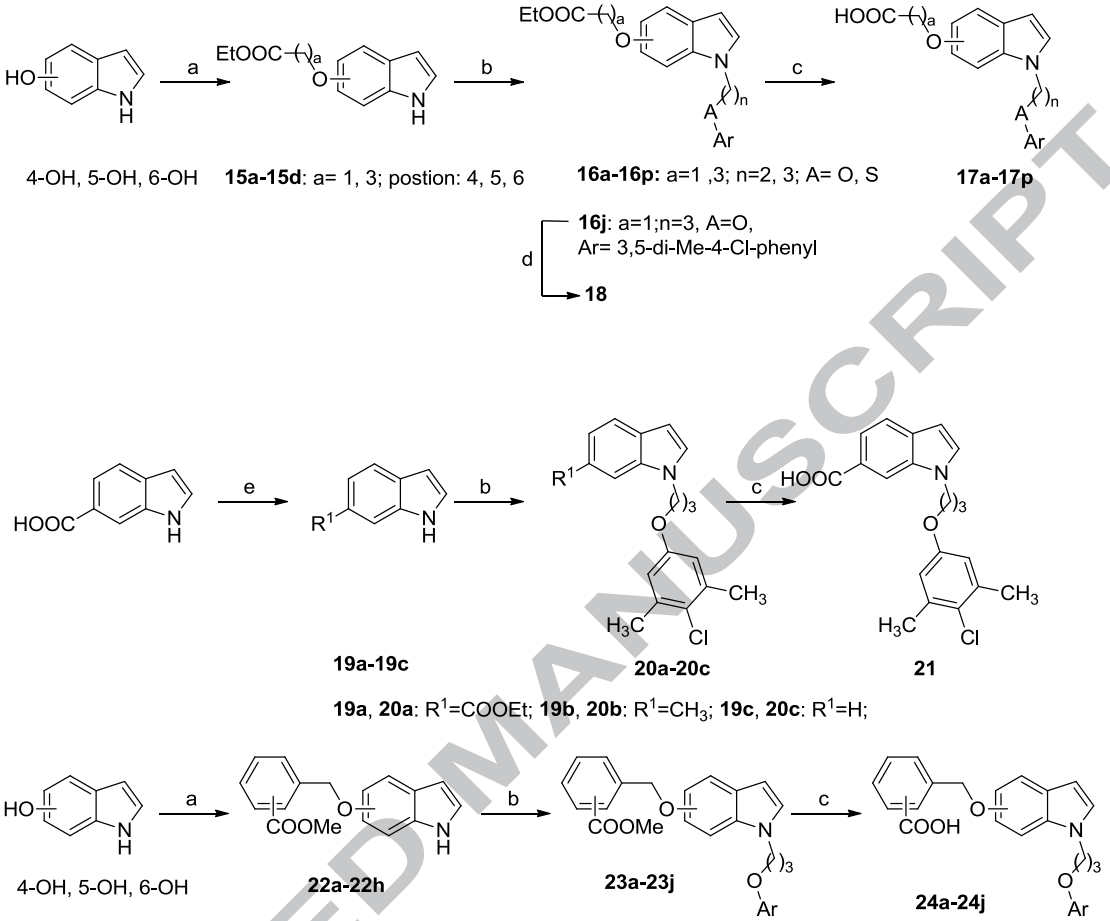

Scheme 2. Synthetic routes of *N*-substituted indole derivatives **17a-17p, 20a-20c, 21 and 24a-24j** Reagents and conditions: (a) $Br(CH_2)_aCOOEt$ (a= 1 or 3) or methyl *o,m,p*-(bromomethyl)benzoate, Cs_2CO_3, MeCN, r.t.; (b) side chains, Cs_2CO_3, MeCN, reflux; (c) LiOH, THF/H_2O, r.t.; (d) $LiAlH_4$, THF, r.t.; (e) $SOCl_2$, EtOH, reflux.

As shown in **Figure 2**, the polar 2-carbamoyl group mismatched the hydrophobic characteristic of P2 pocket and the docking result showed no related interaction with Mcl-1. We hypothesized that this polar group was unnecessary and might have adverse effect on potency. An analogue without 2-carbamoyl group was prepared to verify this hypothesis. According to the data in **Table 1**, compound **17a** (K_i =4.42 μM) show nearly 2-fold increase than the counterpart, which indicated that 2-carbamoyl was not an essential pharmacophore. Follow-up studies reconfirmed the negligible contribution of that group (by comparing **14a-14d** to **17a-17d**). Moreover, the deletion of 2-carbamoyl group improved the solubility of compounds which simplified the purification process (data not show). Significantly, compounds without a carbamoyl group were easily obtained by just three steps, which could facilitate future optimization efforts.

The predicted binding mode represented that the hydrophobic P2 pocket of Mcl-1 was partially occupied by *p*-methoxyphenyl of hit compound **14a**, we assumed that sufficient exploiting of this sub-pocket by introducing steric and hydrophobic groups could be beneficial to potency. Then, the SAR studies of hydrophobic tail were conducted. Initially, removal of para-methoxy group (**17e**) totally deprived the Mcl-1 inhibitory activity, indicating the significant role of substituent groups of distal phenyl. The SAR analysis was done based on a series of analogues with various substituted phenyl on the hydrophobic tail. Installation of simple small groups such as methyl and chlorine (**17f-17i**) exhibited slight decreased potency (K_i varied from 9.89 μM to 12.87 μM) except for the incorporation of 3',5'-di-Me-4'-Cl-phenyl which produced a 5-fold more potent inhibitor **17j** than **14a** (K_i =1.50 μM). Interestingly, this substitution pattern was preferred in several recent publications and considered as anchoring unit of some Mcl-1 inhibitors. [21-24] Several kinds of steric and hydrophobic groups were also introduced into P2 binding moiety and produced 2-fold to 4-fold improvement on binding affinity such as *t*-butyl (**14b**, K_i=1.87 μM), phenoxyl (**14c**, K_i=3.24 μM) and naphthyl (**14d**, K_i=2.57 μM). The tolerance of larger and more hydrophobic groups manifested that the hydrophobic tail was probably positioned at the Mcl-1 deepest hydrophobic P2 pocket as our prediction. The linker length and heteroatom of hydrophobic tail also influenced the binding ability. Based on the molecular modeling, only 3-atoms or 4-atoms linker could properly place the substituted phenyl into the bottom of P2 pocket. Compounds **17k** and **17l** bearded shorten linkers and produced 8-fold and 5-fold reduction compared to counterparts **17b** and **17j** respectively, indicating that the 3-atoms linker was inappropriate. Moreover, replacement of the oxygen on the linker with a more hydrophobic sulfur atom (**17m**) resulted in marginal decrease on potency. In summary, the substitutions on hydrophobic tail and linker length have crucial roles on binding affinity, which should be optimized precisely. In our SAR research, the preferable substitution patterns were 4'-*t*-butyl and 3', 5'-di-Me-4'-Cl and the original linker should be retained.

(**Table 1** should be listed here)

Table 1. The structures and *in vitro* Mcl-1 inhibitory activity of **14a-14d** and **17a-17m**

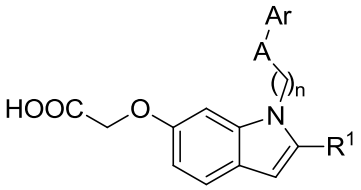

Compd.	R^1	Ar	A	n	Mcl-1 [a] (K_i±SD, μM)
14a	$CONH_2$	4-OCH_3-phenyl	O	3	7.78±1.21
14b	$CONH_2$	4-*t*-Bu-phenyl	O	3	5.38±1.13
14c	$CONH_2$	4-phenoxyphenyl	O	3	4.13±0.44
14d	$CONH_2$	1-Naphthyl	O	3	10.26±0.71
17a	H	4-OCH_3-phenyl	O	3	4.42±0.83
17b	H	4-*t*-Bu-phenyl	O	3	1.87±0.28
17c	H	4-phenoxyphenyl	O	3	3.24±0.57
17d	H	1-Naphthyl	O	3	2.57±0.79
17e	H	phenyl	O	3	>30
17f	H	3-Me-phenyl	O	3	>30
17g	H	3,5-di-Me-phenyl	O	3	12.53±1.80
17h	H	4-Cl-phenyl	O	3	12.87±1.33
17i	H	3-Me-4-Cl-phenyl	O	3	9.89±1.13
17j	H	3,5-di-Me-4-Cl-phenyl	O	3	1.50±0.19
17k	H	4-*t*-Bu-phenyl	O	2	8.19±1.01
17l	H	3,5-di-Me-4-Cl-phenyl	O	2	11.61±2.05
17m	H	4-*t*-Bu-phenyl	S	3	2.38±0.35
Gossypol					0.20±0.05

[a] Values were measured by FP assay for inhibition constant (K_i). The values are the mean ± SD of three independent experiments.

The acidic chain which mimics the conserved Asp of BH3-only peptides was considered as a crucial pharmacophore and further optimization was focused on that. Firstly, adjustment of the attached site (**17j**, **17n** and **17o**) and length of acidic chain (**17j**, **17p** and **21**) produced no obvious discrepancy among these analogs, which showed that this moiety was rather tolerated of modification. Several literatures have reported the extreme importance of acidic group without which the binding affinity for Mcl-1 was totally deprived.[24] Interestingly, our compounds whose carboxyl was masked by ethyl ester (**16j**) or reduced to alcohol (**18**) just exhibited marginal decreased potency. By contrast, compounds **20a-20c** showed no inhibitory activity against Mcl-1. Docking experiments were employed to clarify the different potency of **16j**, **18** and **20a-20c** (*Supplementary information*, **Figure S1**). Their different capacity of forming H-bond with R263 might be the main factor which has impact on binding affinity. Based on our docking results, compounds **16j** and **18** still could form three H-bonds with R263 mediated by oxygen atoms at acidic chain despite the carboxyl group has been masked. By comparison, compound **20a** just

form one H-bond with R263 while **20b** and **20c** form no interactions with R263, which probably result in their deprivation of potency.

(**Table 2** should be listed here)

Table 2. The structures and *in vitro* Mcl-1 inhibitory activity of **16j, 17n-17p, 18-21**

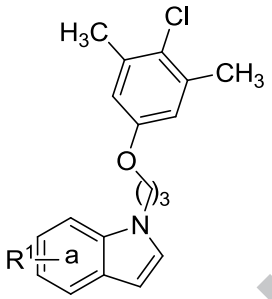

Compd.	a	R^1	Mcl-1 [a] (K_i±SD, μM)
17n	4	OCH_2COOH	2.0±0.34
17o	5	OCH_2COOH	1.49±0.17
17p	6	$O(CH_2)_3COOH$	2.68±0.72
16j	6	OCH_2COOEt	3.37±0.36
18	6	OCH_2CH_2OH	2.10±0.33
20a	6	COOEt	>30
21	6	COOH	3.0±0.84
20b	6	CH_3	>30
20c	6	H	>30
Gossypol			0.20±0.05

[a] Values were measured by FP assay for inhibition constant (K_i). The values are the mean ± SD of three independent experiments.

The substantial increase on potency was still not obtained after the first round optimization, although we indeed achieved a little progress such as 5-fold improved potency. We speculated that the volume of our compounds were too small to occupy the entire Mcl-1 groove effectively, when compared with the natural binding partners (*e.g.* BH3 peptides) or other recently reported inhibitors exemplified by A-1210477 (**5**). [27] Based on the structural data of Mcl-1, the residue of R263 is rather flexible and solvent-exposed, leaving large room for further optimization on acidic chain. In addition, the previous SAR results indicated that modification on this moiety seems to be more tolerated. Consequently, we made more optimizations on the acidic chain. To match the hydrophobic characteristic of Mcl-1 groove, the aliphatic carboxylic acid was replaced by benzoic acid. Rationally, the extra benzene ring is expected to form additional interactions with

surrounding hydrophobic residues while the carboxyl maintains the favorable interactions with R263. Besides, the enlarged size of molecules might restrict the flexible conformations of our molecules, which might be beneficial to potency. Novel indole analogue incorporating with the benzoic acid (**24a**) confirmed this assumption. A sub-micromole level binding affinity (K_i= 0.80 μM) was observed by FP assay, which showed almost 10-fold improvement by comparison with compound **14a**. The attached positions of carboxyl group on phenyl might have influence on potency. As shown in **Table 3**, both the *ortho* (**24a**, **24d**, **24e**, **24i** with K_i= 0.11~0.80 μM) and *meta* (**24b**, **24f**, **24g**, **24j** with K_i= 0.15~0.74 μM) carboxyl group on phenyl have more favorable effect on binding affinity than the *para*-substituted derivatives (**24c**, **24h** with K_i= 1.19, 1.63 μM), which probably due to the different distance and spatial accessibility to R263. Besides, the attached position of acidic chain also had influence on potency. Generally, attaching the acidic chain on C4 (**24i, 24j**) and C5 (**24d-24g**) were more preferable than C6 (**24a-24b**). The most potent compound **24d** (K_i= 0.11 μM) was obtained with 70-fold increased binding affinity than hit compound **14a**, exhibiting higher potency for Mcl-1 than (−)-gossypol (K_i= 0.20 μM) in FP assay. Molecular modeling experiments were employed to explain the improvement of binding affinity. The docking results of **24a**, **24d** and **24i** were depicted in **Figure 3**. The hydrophobic tail inserts into the deep P2 pocket while the indole core occupy the upper P2 pocket, which is consistent with the binding mode of hit compound **14a** (**Figure 1**). Besides, the benzoic acid moiety could form not only charge-charge interactions but also hydrophobic interactions with R263. Specially, **24d** and **24i** could form additional H-bonds with N260 which may make extra contributions on binding affinity. The overlay of **24d** with bound conformation of Bim peptide (**Figure 3D**) showed that compound **24d** could mimic the hotspots h2 and D67 of Bim peptide.

(**Figure 3** should be listed here)

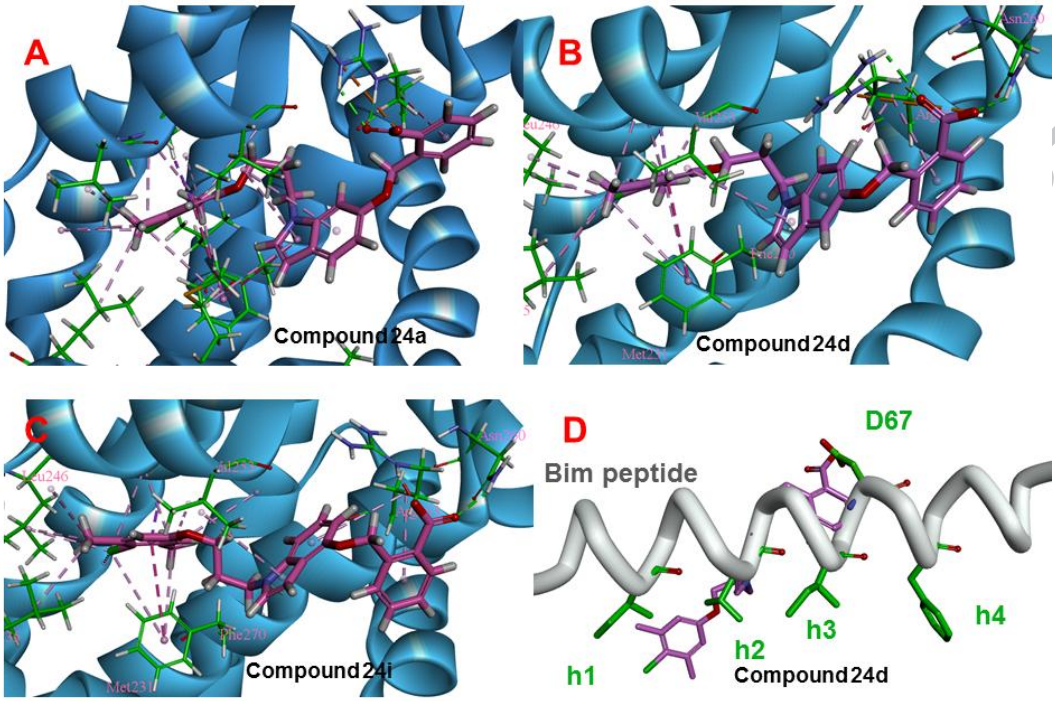

Figure 3. The binding modes of typical compounds **24a** (**A**), **24d** (**B**) and **24i** (**C**) and the overlay of **24d** with bound conformation of Bim peptide (**D**). Pink carbons; heteroatoms colored by atom type; the amino acid side chains interacting with ligand were colored as green. The pink dashed lines present hydrophobic interactions; the orange dashed lines present salt bridges; the green dashed lines present hydrogen bonds. The Bim peptide was colored as offwhite and the hot spots was colored as green and labeled as h1-h4 and D67.

As we can see from **Figure 3A-3C**, the C2 position of indole core is in proximity to the hydrophobic amino acid side chains of M231, V253 and F270. We assumed that introducing additional hydrophobic groups at this position could form more interactions and improve the binding affinity. Consequently, compounds **14e-14i** were prepared to expand our inhibitors (**Table 3**). The results were preliminary yet promising which indicated that C2 is a modifiable position to improve the potency. For instance, with the increase of the volume of R_1, the binding affinity showed rising trend and compound **14h** (K_i= 0.20 μM) obtained 4-fold improvement compared with parental compound **24a** (K_i= 0.80 μM). The docking results showed that compound **14h** could form extra hydrophobic interactions with M231, L235 and V253 mediated by aliphatic ring on C2 as anticipated (*Supplementary information*, **Figure S2**).

Finally, we evaluated the selectivity profile of typical compounds for Bcl-2 protein. The data in **Table 3** indicated that our inhibitors could bind to Bcl-2 as similar potency as Mcl-1. Despite of the structural similarity with Fesik's inhibitor (**1**) and A-1210477 (**5**), our compounds showed no obvious selectivity for Mcl-1. Compared with the Mcl-1 selective inhibitors **1** and **5**, the acidic groups of our inhibitors exhibit more flexibility which probably could adapt to the subtle positional difference of conserved arginine between Mcl-1 and Bcl-2.

In conclusion, a series of novel *N*-substituted indole derivatives as Mcl-1 inhibitors based on an in-house hit LSL-A6 (**14a**) have been designed and synthesized. The related structure-activity relationship was conducted and the most potent compound **24d** which exhibited K_i value of 110 nM for Mcl-1 was obtained. Although the sub-micromole level binding affinity of **24d** might not be expected to confer on-target cellular effects and the selectivity of **24d** is not very specific, [35] this molecule is still a promising lead as the several potential modifiable sites it has. Specially, preliminary data indicated that C2 position of indole core was a promising modifiable position to enhance the potency. The SAR studies and molecular modeling results indicated that all these compounds probably bind with P2 pocket and R263 of Mcl-1 while barely with other hot-spots such as P1, P3 and P4 pockets. Hence, further work will be focused on effectively occupying more hot-spots within BH3 groove and enhance the selectivity for Mcl-1.

(**Table 3** should be listed here)

Table 3. The structures and *in vitro* Mcl-1 inhibitory activity of **24a-24j** and **14e-14h**

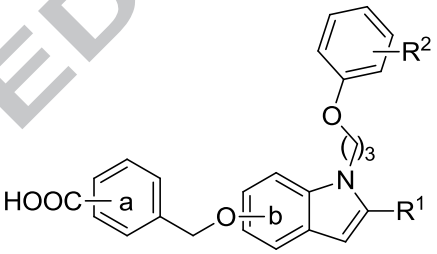

Compd.	a	b	R^1	R^2	Mcl-1 [a] (K_i±SD, μM)	Bcl-2 [a] (K_i±SD, μM)
24a	2’	6	H	3,5-di-Me-4-Cl	0.80±0.15	1.05±0.14
24b	3’	6	H	3,5-di-Me-4-Cl	0.74±0.09	1.19±0.21
24c	4’	6	H	3,5-di-Me-4-Cl	1.19±0.21	1.24±0.28
24d	2’	5	H	3,5-di-Me-4-Cl	0.11±0.0058	0.76±0.05
24e	2’	5	H	4-*t*-Bu	0.31±0.04	0.17±0.02
24f	3’	5	H	3,5-di-Me-4-Cl	0.20±0.04	0.41±0.06
24g	3’	5	H	4-*t*-Bu	0.25±0.02	0.47±0.03
24h	4’	5	H	3,5-di-Me-4-Cl	1.63±0.20	1.41±0.23
24i	2’	4	H	3,5-di-Me-4-Cl	0.14±0.01	0.23±0.03
24j	3’	4	H	3,5-di-Me-4-Cl	0.15±0.01	0.14±0.02
14e	2’	6	$CONH_2$	3,5-di-Me-4-Cl	0.95±0.04	0.85±0.04
14f	2’	6	$CONHCH_3$	3,5-di-Me-4-Cl	0.89±0.09	0.81±0.01
14g	2’	6	$CONH(CH_3)_2$	3,5-di-Me-4-Cl	0.57±0.07	0.73±0.10
14h	2’	6		3,5-di-Me-4-Cl	0.20±0.01	0.27±0.03
14i	2’	6		4-*t*-Bu	0.36±0.06	0.15±0.02

Gossypol	0.20±0.05	0.42±0.11

[a] Values were measured by FP assay for inhibition constant (K_i). The values are the mean ± SD of three independent experiments.

Supplementary information

All the experimental protocols (chemistry, biological, computational protocols) and spectrums of target compounds are detailed in *Supplementary information*.

Acknowledgment

We thank Dr. Ting song (Dalian University of Technology) for the binding assay for Mcl-1 protein and Jian Wang (Shenyang Pharmaceutical University) for the insightful discussions on molecular docking research. The work was supported by National Natural Science Foundation of China(Grant No. 8173293).

Reference

1. Hanahan D.; Weinberg R.A. *Cell*. **2011**, *144*, 646.
2. Hanahan D.; Weinberg R.A. *Cell*. **2000**, *100*, 57.
3. Adams J.M.; Cory S. *Oncogene*. **2007**, *26*, 1324.
4. Czabotar P.E.; Lessene G.; Strasser A.; Adams J.M. *Nat Rev Mol Cell Biol*. **2014**, *15*, 49.
5. Kvansakul M.; Hinds M.G. *Apoptosis*. **2015**, *20*, 136.
6. Igney F.H.; Krammer P.H. *Nat Rev Cancer*. **2002**, *2*, 277.
7. Placzek W.J.; Wei J.; Kitada S.; Zhai D.; Reed J.C.; Pellecchia M. *Cell Death Dis*. **2010**, *1*, e40.
8. Oltersdorf T.; Elmore S.W.; Shoemaker A.R.; Armstrong R.C.; Augeri D.J.; Belli B.A.; Bruncko M.; Deckwerth T.L.; Dinges J.; Hajduk P.J.; Joseph M.K.; Kitada S.; Korsmeyer S.J.; Kunzer A.R.; Letai A.; Li C.; Mitten M.J.; Nettesheim D.G.; Ng S.; Nimmer P.M.; O'Connor J.M.; Oleksijew A.; Petros A.M.; Reed J.C.; Shen W.; Tahir S.K.; Thompson C.B.; Tomaselli K.J.; Wang B.; Wendt M.D.; Zhang H.; Fesik S.W.; Rosenberg S.H. *Nature*. **2005**, *435*, 677.
9. Tse C.; Shoemaker A.R.; Adickes J.; Anderson M.G.; Chen J.; Jin S.; Johnson E.F.; Marsh K.C.; Mitten M.J.; Nimmer P.; Roberts L.; Tahir S.K.; Xiao Y.; Yang X.; Zhang H.; Fesik S.; Rosenberg S.H.; Elmore S.W. *Cancer Res*. **2008**, *68*, 3421.
10. Souers A.J.; Leverson J.D.; Boghaert E.R.; Ackler S.L.; Catron N.D.; Chen J.; Dayton B.D.; Ding H.; Enschede S.H.; Fairbrother W.J.; Huang D.C.; Hymowitz S.G.; Jin S.; Khaw S.L.; Kovar P.J.; Lam L.T.; Lee J.; Maecker H.L.; Marsh K.C.; Mason K.D.; Mitten M.J.; Nimmer P.M.; Oleksijew A.; Park C.H.; Park C.M.; Phillips D.C.; Roberts A.W.; Sampath D.; Seymour J.F.; Smith M.L.; Sullivan G.M.; Tahir S.K.; Tse C.; Wendt M.D.; Xiao Y.; Xue J.C.; Zhang H.; Humerickhouse R.A.; Rosenberg S.H.; Elmore S.W. *Nat Med*. **2013**, *19*, 202.
11. Cang S.; Iragavarapu C.; Savooji J.; Song Y.; Liu D. *J Hematol Oncol*. **2015**, *8*, 129.
12. Konopleva M.; Contractor R.; Tsao T.; Samudio I.; Ruvolo P.P.; Kitada S.; Deng X.; Zhai D.; Shi Y.X.; Sneed T.; Verhaegen M.; Soengas M.; Ruvolo V.R.; McQueen T.; Schober W.D.; Watt J.C.; Jiffar T.; Ling X.; Marini F.C.; Harris D.; Dietrich M.; Estrov Z.; McCubrey J.; May W.S.; Reed J.C.; Andreeff M. *Cancer Cell*. **2006**, *10*, 375.
13. Niu X.; Zhao J.; Ma J.; Xie C.; Edwards H.; Wang G.; Caldwell J.T.; Xiang S.; Zhang X.; Chu R.; Wang Z.J.; Lin H.; Taub J.W.; Ge Y. *Clin Cancer Res*. **2016**, *22*, 4440.
14. Wang B.; Ni Z.; Dai X.; Qin L.; Li X.; Xu L.; Lian J.; He F. *Mol Cancer*. **2014**, *13*, 98.

15. Mazumder S.; Choudhary G.S.; Al-Harbi S.; Almasan A. *Cancer Res*. **2012**, *72*, 3069.
16. Wei S.H.; Dong K.; Lin F.; Wang X.; Li B.; Shen J.J.; Zhang Q.; Wang R.; Zhang H.Z. *Cancer Chemother Pharmacol*. **2008**, *62*, 1055.
17. Phillips D.C.; Xiao Y.; Lam L.T.; Litvinovich E.; Roberts-Rapp L.; Souers A.J.; Leverson J.D. *Blood Cancer J*. **2015**, *5*, e368.
18. Zhao X.; Zhong H.; Wang R.; Liu D.; Waxman S.; Zhao L.X.; Jing Y.K. *Oncotarget*. **2015**, *6*, 5582.
19. Besbes S.; Pocard M.; Mirshahi M.; Billard C. *Crit Rev Oncol Hematol*. **2016**, *100*, 32.
20. Pelz N.F.; Bian Z.; Zhao B.; Shaw S.; Tarr J.C.; Belmar J.; Gregg C.; Camper D.V.; Goodwin C.M.; Arnold A.L.; Sensintaffar J.L.; Friberg A.; Rossanese O.W.; Lee T.; Olejniczak E.T.; Fesik S.W. *J Med Chem*. **2016**, *59*, 2054.
21. Lanning M.E.; Yu W.; Yap J.L.; Chauhan J.; Chen L.; Whiting E.; Pidugu L.S.; Atkinson T.; Bailey H.; Li W.; Roth B.M.; Hynicka L.; Chesko K.; Toth E.A.; Shapiro P.; MacKerell A.D., Jr.; Wilder P.T.; Fletcher S. *Eur J Med Chem*. **2016**, *113*, 273.
22. Drennen B.; Scheenstra J.A.; Yap J.L.; Chen L.; Lanning M.E.; Roth B.M.; Wilder P.T.; Fletcher S. *ChemMedChem*. **2016**, *11*, 827.
23. Chen L.; Wilder P.T.; Drennen B.; Tran J.; Roth B.M.; Chesko K.; Shapiro P.; Fletcher S. *Org Biomol Chem*. **2016**, *14*, 5505.
24. Friberg A.; Vigil D.; Zhao B.; Daniels R.N.; Burke J.P.; Garcia-Barrantes P.M.; Camper D.; Chauder B.A.; Lee T.; Olejniczak E.T.; Fesik S.W. *J Med Chem*. **2013**, *56*, 15.
25. Wan Y.; Wu S.; Xiao G.; Liu T.; Hou X.; Chen C.; Guan P.; Yang X.; Fang H. *Bioorg Med Chem*. **2015**, *23*, 1994.
26. Leverson J.D.; Zhang H.; Chen J.; Tahir S.K.; Phillips D.C.; Xue J.; Nimmer P.; Jin S.; Smith M.; Xiao Y.; Kovar P.; Tanaka A.; Bruncko M.; Sheppard G.S.; Wang L.; Gierke S.; Kategaya L.; Anderson D.J.; Wong C.; Eastham-Anderson J.; Ludlam M.J.; Sampath D.; Fairbrother W.J.; Wertz I.; Rosenberg S.H.; Tse C.; Elmore S.W.; Souers A.J. *Cell Death Dis*. **2015**, *6*, e1590.
27. Bruncko M.; Wang L.; Sheppard G.S.; Phillips D.C.; Tahir S.K.; Xue J.; Erickson S.; Fidanze S.; Fry E.; Hasvold L.; Jenkins G.J.; Jin S.; Judge R.A.; Kovar P.J.; Madar D.; Nimmer P.; Park C.; Petros A.M.; Rosenberg S.H.; Smith M.L.; Song X.; Sun C.; Tao Z.F.; Wang X.; Xiao Y.; Zhang H.; Tse C.; Leverson J.D.; Elmore S.W.; Souers A.J. *J Med Chem*. **2015**, *58*, 2180.
28. Richard D.J.; Lena R.; Bannister T.; Blake N.; Pierceall W.E.; Carlson N.E.; Keller C.E.; Koenig M.; He Y.; Minond D.; Mishra J.; Cameron M.; Spicer T.; Hodder P.; Cardone M.H. *Bioorg Med Chem*. **2013**, *21*, 6642.
29. Wang G.; Nikolovska-Coleska Z.; Yang C.Y.; Wang R.; Tang G.; Guo J.; Shangary S.; Qiu S.; Gao W.; Yang D.; Meagher J.; Stuckey J.; Krajewski K.; Jiang S.; Roller P.P.; Abaan H.O.; Tomita Y.; Wang S. *J Med Chem*. **2006**, *49*, 6139.
30. Abulwerdi F.A.; Liao C.; Mady A.S.; Gavin J.; Shen C.; Cierpicki T.; Stuckey J.A.; Showalter H.D.; Nikolovska-Coleska Z. *J Med Chem*. **2014**, *57*, 4111.
31. Kotschy A.; Szlavik Z.; Murray J.; Davidson J.; Maragno A.L.; Le Toumelin-Braizat G.; Chanrion M.; Kelly G.L.; Gong J.N.; Moujalled D.M.; Bruno A.; Csekei M.; Paczal A.; Szabo Z.B.; Sipos S.; Radics G.; Proszenyak A.; Balint B.; Ondi L.; Blasko G.; Robertson A.; Surgenor A.; Dokurno P.; Chen I.; Matassova N.; Smith J.; Pedder C.; Graham C.; Studeny A.; Lysiak-Auvity G.; Girard A.M.; Grave F.; Segal D.; Riffkin C.D.; Pomilio G.; Galbraith L.C.; Aubrey B.J.; Brennan M.S.; Herold M.J.; Chang C.; Guasconi G.; Cauquil N.; Melchiore F.; Guigal-Stephan N.; Lockhart B.; Colland F.; Hickman J.A.; Roberts A.W.; Huang D.C.; Wei A.H.; Strasser A.; Lessene G.; Geneste O. *Nature*. **2016**, *538*, 477.
32. Akcay G.; Belmonte M.A.; Aquila B.; Chuaqui C.; Hird A.W.; Lamb M.L.; Rawlins P.B.; Su N.; Tentarelli S.; Grimster N.P.; Su Q. *Nat Chem Biol*. **2016**, *12*, 931.
33. Zhang Z.; Wu G.; Xie F.; Song T.; Chang X. *J Med Chem*. **2011**, *54*, 1101.
34. Khurana L.; Ali H.I.; Olszewska T.; Ahn K.H.; Damaraju A.; Kendall D.A.; Lu D. *J Med Chem*. **2014**, *57*, 3040.
35. Belmar J.; Fesik S.W. *Pharmacol Ther*. **2015**, *145*, 76.

*Graphical Abstract

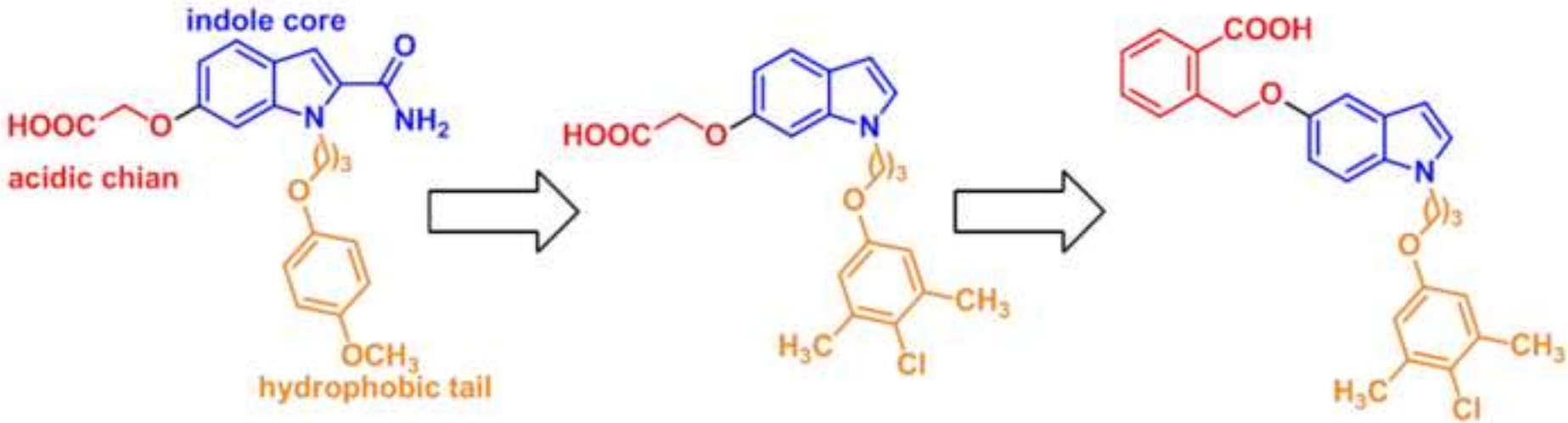

Hit compound (14a)
Mcl-1 K_i= 7.78 μM

Compound 17j
Mcl-1 K_i= 1.50 μM

Compound 24d
Mcl-1 K_i= 0.11 μM